Earth Systems and Climate Change Hub

National Environmental Science Programme

A comprehensive report of model systematic errors in the latest ACCESS climate models

Hongyan Zhu, Christian Jakob, Yimin Ma, Rob Warren, Abhik Santra, Soner Yorgun and Zhian Sun

June 2018

Earth Systems and Climate Change Hub Report No. 3

Australian Government

National Environmental Science Programme

The Earth Systems and Climate Change Hub is supported by funding through the Australian Government's National Environmental Science Program. The Hub is hosted by the Commonwealth Scientific and Industrial Research Organisation (CSIRO), and is a partnership between CSIRO, Bureau of Meteorology, Australian National University, Monash University, University of Melbourne, University of New South Wales and University of Tasmania. The role of the Hub is to ensure that Australia's policies and management decisions are effectively informed by Earth systems and climate change science, now and into the future. For more information visit www.nespclimate.com.au.

Copyright

© Bureau of Meteorology 2018

A comprehensive report of model systematic errors in the latest ACCESS climate models is licensed by the Bureau of Meteorology for use under a Creative Commons Attribution 4.0 Australia licence. For licence conditions see https://creativecommons.org/licenses/by/4.0/

Citation

Zhu H, Jakob C, Ma Y, Warren, R, Santra A, Yorgen S and Sun Z. 2018. *A comprehensive report of model systematic errors in the latest ACCESS climate models*. Earth Systems and Climate Change Hub Report No. 3, NESP Earth Systems and Climate Change Hub, Australia.

Contact

Enquiries regarding this report should be addressed to:

Dr Hongyan Zhu
Bureau of Meteorology
hongyan.zhu@bom.gov.au

Published June 2018

This report is available for download from the Earth Systems and Climate Change Hub website at www.nespclimate.com.au.

Important disclaimer

The National Environmental Science Program (NESP) Earth Systems and Climate Change (ESCC) Hub advises that the information contained in this publication comprises general statements based on scientific research. The reader is advised and needs to be aware that such information may be incomplete or unable to be used in any specific situation. No reliance or actions must therefore be made on that information without seeking prior expert professional, scientific and technical advice. To the extent permitted by law, the NESP ESCC Hub (including its host organisation, employees, partners and consultants) excludes all liability to any person for any consequences, including but not limited to all losses, damages, costs, expenses and any other compensation, arising directly or indirectly from using this publication (in part or in whole) and any information or material contained in it.

The ESCC Hub is committed to providing web accessible content wherever possible. If you are having difficulties with accessing this document, please contact info@nespclimate.com.au.

Contents

Figures

Tables

Acknowledgements

We thank Dr Tony Hirst and Dr Gary Dietachmayer for their constructive suggestions and comments which greatly improved the manuscript. We would also like to show our gratitude to Dr Harun Rashid and Dr Huqing Zhang for helping us with the internal review of this work. This work has been supported through funding from the Earth Systems and Climate Change Hub of the Australian Government's National Environmental Science Program.

Report summary

At a glance

Building on a preliminary evaluation which identified temperature, rainfall, radiation and circulation biases in the ACCESS climate model, Earth Systems and Climate Change Hub researchers conducted further simulations to understand the cause of the identified biases and the potential modifications required to improve the ACCESS climate model. This will improve the ability of ACCESS to realistically simulate our climate, resulting in better climate information to inform decisions and policy.

The ACCESS climate model

The Australian Community Climate and Earth System Simulator (ACCESS) is a comprehensive climate model comprised of atmosphere, ocean, land surface and sea-ice models. These models are 'coupled' to more realistically represent the climate system.

While ACCESS is among the top performing climate models internationally, like all models it has different biases (also referred to as model systematic errors) in its simulation of the climate. To improve the performance of the model, these biases in key climate variables need to be documented, the processes causing them need to be identified and modifications to improve the biases need to be tested. This will allow improvements in how the climate variables are represented in the model, so simulations better match the observed climate.

Assessing the ACCESS atmospheric model

Preliminary evaluation of the ACCESS model conducted by Rashid et al (2017; see Earth Systems and Climate Change Hub Report 1) showed that, overall, the high-resolution atmospheric model does a better job of realistically simulating the major surface and atmospheric climate features than the low-resolution version. However, the preliminary evaluation found that there were still significant biases that need to be investigated further to understand their causes.

Building on these preliminary findings, Earth System and Climate Change Hub researchers conducted further simulations on the latest ACCESS climate model to understand the causes of biases identified. These investigations focused on the simulation of tropical rainfall including the diurnal (daily) rainfall cycle and Madden-Julian Oscillation (MJO); surface heat fluxes; surface wind speeds and radiation fluxes.

In this evaluation, model systematic errors in the recent versions of the ACCESS climate model using the GA7 and GA7.1 atmospheric model physics are compared and documented. The ACCESS Singular Column Model (SCM) (with the GA6 model physics package) is also used in this evaluation

to identify the model systematic errors and test possible modifications to model representations of tropical convection to reduce those errors.

Evaluation findings

Rainfall biases

The representation of rainfall in ACCESS models is generally wetter than observed over the tropical western Pacific and Indian Oceans, and drier than observed over the Maritime Continent (the region between the Indian and Pacific Oceans). This evaluation found that by increasing model resolution, both these biases are reduced. This also leads to improved Madden-Julian Oscillation model simulations.

Diurnal rainfall cycle biases

The diurnal cycle of rainfall over tropical land is not well represented in the model. A modification to the parameterised convection scheme by implementing the convective memory scheme resulted in a reduction in the drying bias over the Maritime Continent and, due to the interconnections through the Walker Circulation, a reduction to the wet biases in the Indian Ocean and West Pacific Ocean. The representation of diurnal rainfall cycles over tropical land also improved.

Surface heat fluxes and surface wind speeds biases

Surface heat fluxes and surface wind speeds show consistency with other climate models. The high-resolution model performs better in representing global energy exchanges at the surface and surface winds.

Biases in radiation and heat fluxes

Southern Ocean shortwave radiation biases in the ACCESS climate model with the GA7.1 physics package are much improved compared to previous versions of the model. This may also lead to improvements in sea surface temperature simulations.

Increased spatial resolution reduces the relatively large positive biases occurring in lower resolution models in sensible and latent heat flux in the polar regions, however biases are increased in the equatorial and southern mid-latitude oceans.

ACCESS Singular Column Model experiments

The ACCESS SCM is used in this evaluation to test possible modifications to the model representation of tropical convections with an aim to reduce model systematic errors. Using ACCESS SCM to examine the modifications to the elements of deep convection representation in the ACCESS model showed that implementing a different trigger to the convection reduces the intermittency of rainfall. A preliminary investigation using ACCESS SCM was also undertaken to determine the potential cause for the wet bias over the tropical ocean, and the role of shallow convection in the representation of water transport from the sub-tropics into the tropics. Due to the

lack of the large-scale circulation feedbacks, the SCM experiments require further investigation using a full climate model.

Next steps

Although modifications to the convection scheme in this evaluation resulted in improvements in the representation of the diurnal rainfall and the reduction in rainfall biases, some rainfall biases associated with the model variability still persist. Future investigations will be conducted to further improve the model biases and its impacts will be documented.

The modifications to deep convection and shallow convection conducted with the ACCESS SCM model is currently being tested using a full climate model.

1. Introduction

This report presents a comprehensive documentation of model systematic errors in the atmospheric component of the ACCESS climate model using the two most recent atmospheric physics packages, the Global Atmosphere 7.0 (GA7) and 7.1 (GA7.1) model physics (Walters et.al. 2017). GA7.1 is expected to be used in the ACCESS-CM2 coupled climate model to be utilised for CMIP6. The present evaluation is mainly focused in the following areas: the simulation of tropical rainfall including spatial biases and realism of the diurnal cycle, the Madden-Julian Oscillation (MJO), surface heat fluxes, surface wind speeds and radiation fluxes. Also sensitivities to some modifications of the convection scheme are explored.

In this report, the ACCESS Singular Column Model (SCM) with the previous GA6 model physics is also used to identify and test possible modifications to the model representation of tropical convection with the aim to reduce model systematic errors. The SCM simulations are used to study the model sensitivities to the convective entrainment, cloud base parcel properties, cloud base mass-flux closures, convection trigger and settings of shallow convection.

The report is organised as follows. The UM model and data used for model evaluation are described in Section 2. Comprehensive evaluations of model systematic error for the latest ACCESS climate model are discussed in Section 3. In Section 4, sensitivities to convection scheme settings using ACCESS SCM are presented. Conclusions and discussion are contained in the final section.

2. Models description and data

For the evaluation, simulations using the atmospheric component of the ACCESS climate model with alternatively the GA7 and GA7.1 model physics packages (Walters et.al. 2017) are conducted. An experimental protocol conforming to the style of the Atmospheric Model Intercomparison Project (AMIP) (Gates et. al., 1998) is adopted, where the atmospheric model is run with prescribed observed monthly and interannually varying sea surface temperature and sea ice extent. For both the GA7 and GA7.1 cases, simulations with two horizontal model resolution, N96 and N216, about 135 and 60 km grid spacing respectively, are carried out with 85 vertical levels, and the details of the experiments are detailed in Table.1. The model uses a modified mass flux convection scheme based on Gregory and Rowntree (1990).

The model uses the prognostic cloud fraction and prognostic condensate (PC2) scheme of Wilson et al. (2008). For the boundary layer scheme, turbulent fluxes of heat, moisture and horizontal momentum in the boundary layer are represented by a first-order K profile closure as described by Lock et al. (2000). Model radiation is represented by a modified version of Edwards and Slingo (1996) scheme based on rigorous solution of the two-stream scattering equations including partial cloud cover. The climate model simulations use observed daily SST and sea ice distributions.

Model	Resolution	Time period
GA7	N96	1989-2008
GA7	N216	2003-2006
GA7.1	N96	1989-2008
GA7.1	N216	2003-2006

Table 1. The experiment lists for the AMIP experiment with GA7 and GA7.1 model physics.

The GA7.0 physics package includes a number of incremental developments and targeted improvements over GA6.0 including deficiencies in the model's numerical conservation. These changes include further developments in the model's microphysics and incremental improvements to the implementation of the dynamical core. In combination with the bottom-up developments, these changes result in some reduction in some of the model biases, namely rainfall deficits over India during the South Asian monsoon, temperature and humidity biases in the 20 tropical tropopause layer, and surface flux biases over the Southern Ocean (Walters et. al., 2017).

In addition to the improvements in GA7, GA7.1 reduces an overly negative anthropogenic aerosol effective radiative forcing in GA7.0, whilst maintaining the quality of simulations of the present-day climate. The differences between GA7.1 and GA7.0 model physics are:

1. A new parametrisation of spectral dispersion for the cloud droplet size distribution following Liu et al. (2008). This parametrises the impact of the droplet number (and hence the aerosol loading) on the dispersion relation, as opposed to 15 the simpler approach adopted in GA7.0, in which the spectral dispersion in continental and maritime clouds is specified according to the model's land sea mask
2. An update to the complex refractive index of black carbon from 1:75-0:44i to the more recent estimate of 1:85-0:71i;
3. Inclusion of more detailed look-up tables for aerosol optical properties in UKCA-Radaer, enabling more accurate spectral resolution of aerosol solar absorption;
4. Replacement of the climatological oceanic dimethlysulphide (DMS) concentration of Kettle et al. (1999) with the updated climatology of Lana et al. (2011);
5. Multiplicative scaling of the parametrised marine emission of DMS in GLOMAP-mode by (1+0:7), where the factor 0.7 is designed to account for a missing source of primary marine organic aerosol in GLOMAP-mode;
6. Several improvements to the calculation of the TKE data passed to UKCA-Activate: (i) an explicit bug in the level indexing was corrected; (ii) the minimum value of TKE used was reduced by an order of magnitude and (iii) an explicit estimate of TKE in cumulus clouds was introduced;
7. Retuning of the parameters mp_dz_scal and cca_sh_knob back to their originally proposed values of 2.0 and 0.5 respectively.

Model simulations are evaluated against a range of climatic reanalysis and observational data sets. These datasets for verification in this report are the GPCP daily precipitation (Huffman et al., 2001); TRMM 3 hourly precipitation (Huffman et al., 2007) ; NCEP-DOE AMIP-II reanalysis data (NCEP2,Kanamitsu et al. 2002); Modern-Era Retrospective Analysis for Research and Applications project (MERRA, Rienecker et al. 2011); ECMWF ERA-Interim archive reanalyses (ERA-INT, Berrisford et al. 2009); ECMWF ERA-40 reanalyses (ERA-40,Uppala et al. 2005). The global climatology of inter-annually varying air–sea flux data set (COREv2, Large and Yeager 2009); NCEP Climate Forecast System Reanalysis (CFSR, Saha et al. 2010); and the Japanese 25-year Reanalysis (JRA25, Onogi et al. 2007). In addition, an observational shortwave radiation dataset, the NASA GEWEX Surface Radiation Budget (SRB, https://gewex-srb.larc.nasa.gov/common/php/SRB_about.php), is also utilised for evaluation.

A set of case studies for use with the Single Column Model (SCM) version of the Unified Model (UM) is set up. These include the versions of the TOGA-COARE and TWP-ICE cases for studying deep and shallow convection.

3. AMIP experiment Results

3.1 Tropical rainfall biases and MJO simulation.

Climate models face a significant challenge in the realistic simulations of rainfall climatology. The rainfall bias for the latest GA7 and GA7.1 model are compared in Figure.1a and b with dry bias over the Maritime Continent (MC) region and wet bias over the western Indian Ocean and western Pacific regions. A dry bias also exists in the north Australia and Indian monsoon region. The difference of average rainfall rate between GA7 and GA7.1 model are neutral with no obvious improvement (See Figure 1c).

The MC is a region where global climate models struggle to realistically represent the spatial distribution of rainfall and its variability (Jourdan et al. 2013). The deficient rainfall over the MC could be a driver for other systematic errors, such as the excess precipitation over the western Indian Ocean. The MC dry bias has been persistent in recent global versions of UM. Biases in rainfall over the MC region have also been reported to adversely affect simulation of the eastward propagation of the MJO across the region (e.g., Neale and Slingo, 2002; Klingamann and Woolnough, 2014).

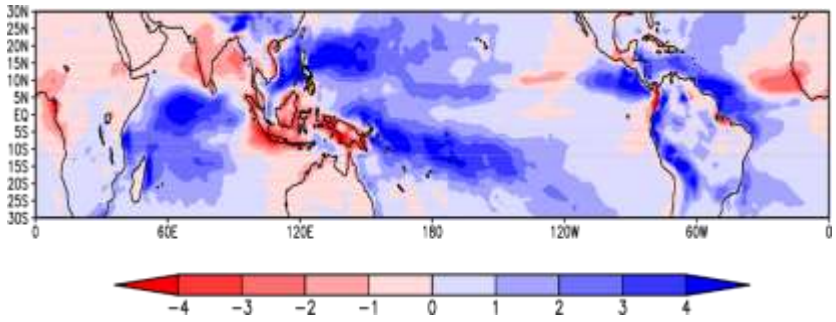

(a)

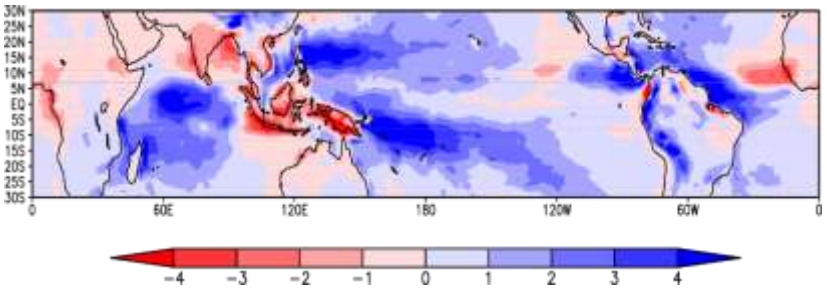

(b)

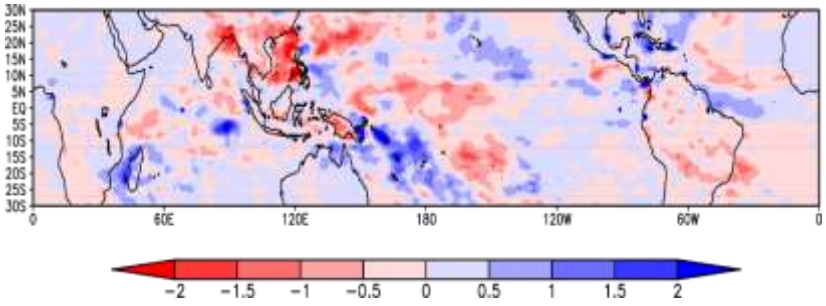

(c)

Figure 1 Annual mean rainfall bias (mm/day) with respect to the GPCP rainfall observations in a low resolution (N96) version of the ACCESS model with GA7 (a) and GA7.1 (b) model physics. (c) shows the difference of the annual mean rainfall rates (mm/day) between the above two simulations. (1989-1998).

Rainfall bias is sensitive to the model resolution. With increased resolution (N216), the modelled rainfall increases mainly over the MC regions (See Figure 2). Due to teleconnections through the Walker circulation, the wet biases over the Indian Ocean and Western Pacific regions have been reduced. Increased resolution also helps to reduce the model dry bias for the Indian Monsoon region.

With the improvement of the mean precipitation distribution in the MC, the eastward propagation of organized convection associated with MJO has also been improved. To demonstrate the ability of the model to simulate eastward propagating intraseasonal variability, we calculate the lead-lag OLR correlation coefficients between 20-100 days bandpass filtered data from a central Indian Ocean time series and the associated 10oN-10oS averaged fields at all longitudes (Figure 3). For the experiment with N96 resolution, convection fails to propagate eastward from the Indian Ocean. In the experiment with N216 resolution, with the improvement of the mean precipitation distribution in the MC region, the model exhibits slightly improved eastward propagation across the Indian and the west Pacific Oceans, but still needing more improvement comparing to the observation (Figure 3c).

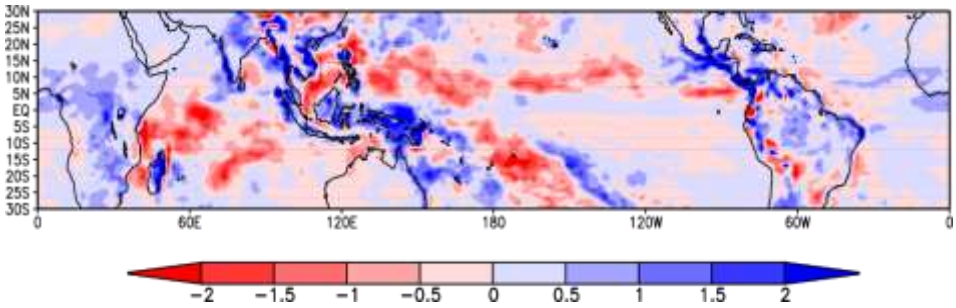

Figure 2 For GA7 model, the annual mean rainfall difference (mm/day) between N216 and N96 simulations. (2003-2006)

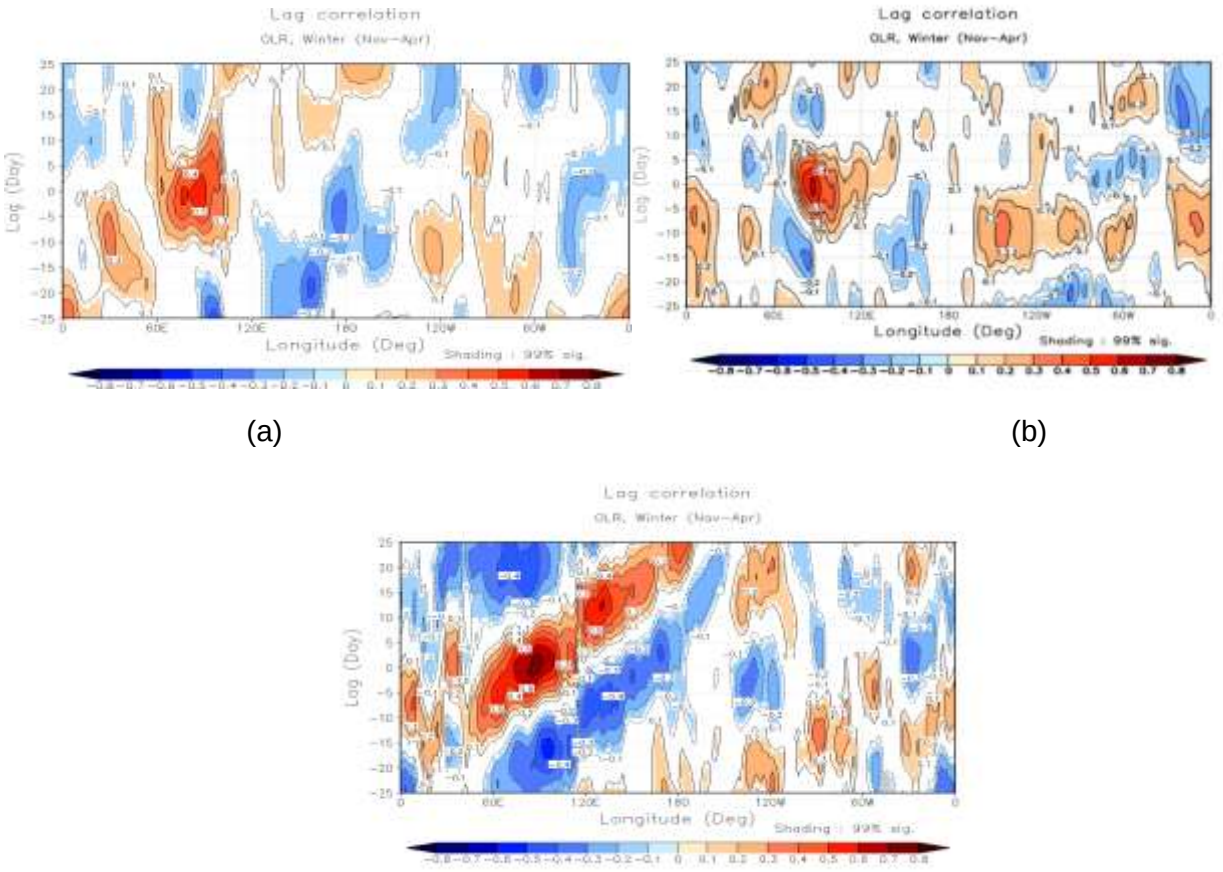

Figure 3 For GA7 model, the lag correlation of equatorial intraseasonal OLR onto a reference zonal OLR time series at 90E in (a) N96 resolution, (b) N216 resolution and (c) observation.

A similar sensitivity to resolution is also observed in GA7.1 model. Figure 4 shows the rainfall difference between N216 model and N96 model and the lead-lag bandpass filtered OLR correlation coefficients are presented in Figure 5. With increased resolution, the rainfall rate increases over MC region and north Australia. As a result, the model shows more persistent eastwards propagating convection cross central Indian Ocean region and MC region.

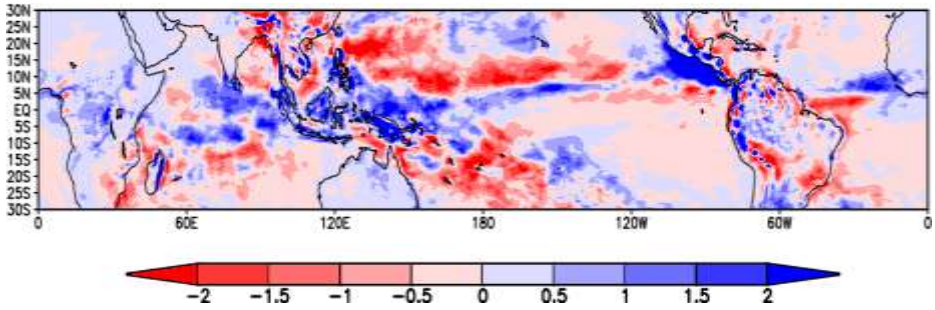

Figure 4 For GA7.1 model, the difference in annual mean precipitation (mm/day) between the high- and low-resolution versions (N216 and N96, respectively).

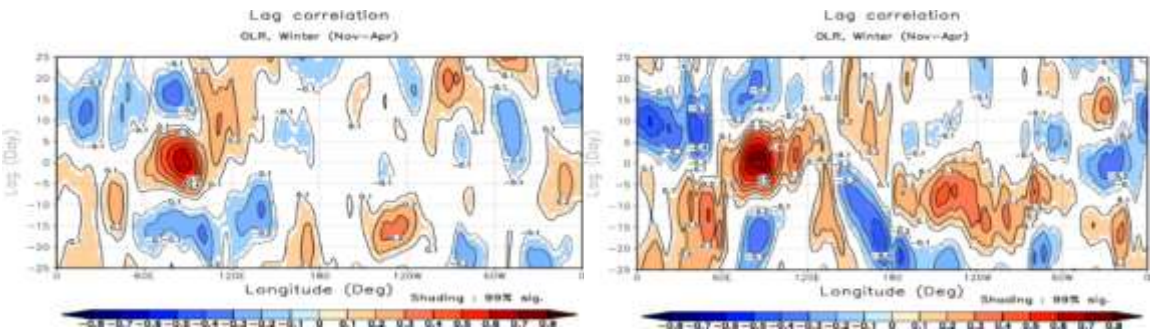

Figure 5 For GA7.1 model, the lag correlation of equatorial intraseasonal OLR onto a reference zonal OLR time series at 90E in the simulations with N96 resolution (left panel) and N216 resolution (right panel).

3.2 Diurnal cycle

The Met Office Unified Model has been shown to have considerable difficulty in capturing the observed phase of the diurnal cycle in convection, which suggests some fundamental difficulties in the model's physical parametrisations (Yang and Slingo 2001). To evaluate the simulation of diurnal cycle, we use 3 hourly TRMM data as the source of comparative observations. Figure 6 compares the diurnal cycle of rainfall rate for the GA7 model with N96 and N216 resolutions for the Borneo Island (defined as 113°–127° E, 5° S–2 ° N, land only).

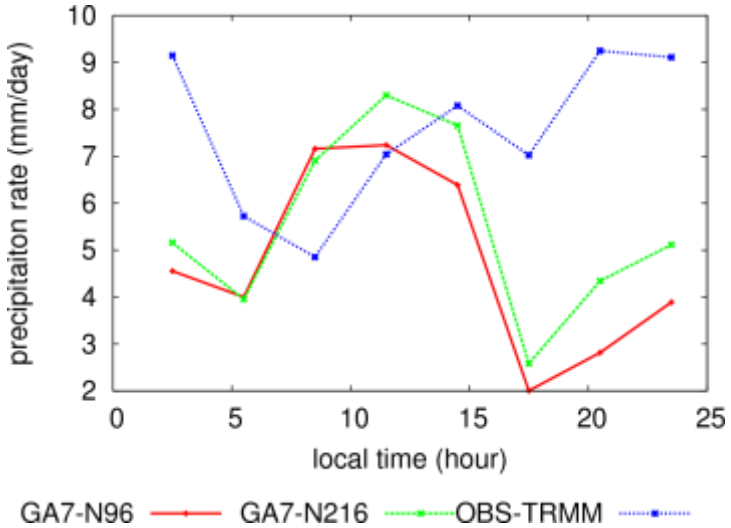

Figure 6 For GA.7 model, diurnal cycles of the rainfall rate (mm/day) over the Borneo Island with N96 and N216 resolutions, comparing against TRMM observations.

Observation shows that rainfall rate has the minimum in the morning around 8 am when rainfall mainly occurs over the ocean surrounding the island (Figure 7 top left). The rainfall starts to increase in the afternoon and reaches its maximum in the late evening and early morning. In GA7 model with N96 resolution, the rainfall rates reaches the maximum in the morning around 10am presumably due to the CAPE closure setting in the convection scheme, which is designed to release the convective instability whenever the instability is available. The rainfall rate minimum occurs in the afternoon around 5pm. The observed convection tends to accumulate the instability, and then rains

in the late afternoon and evening when the convective instability reaches the maximum. The modelled rainfall rates increases over the night, but the amplitude is much weaker compared to the observations. The N216 model has similar diurnal cycle of rain to the N96 model, but the amplitudes are higher as a result of the higher resolution.

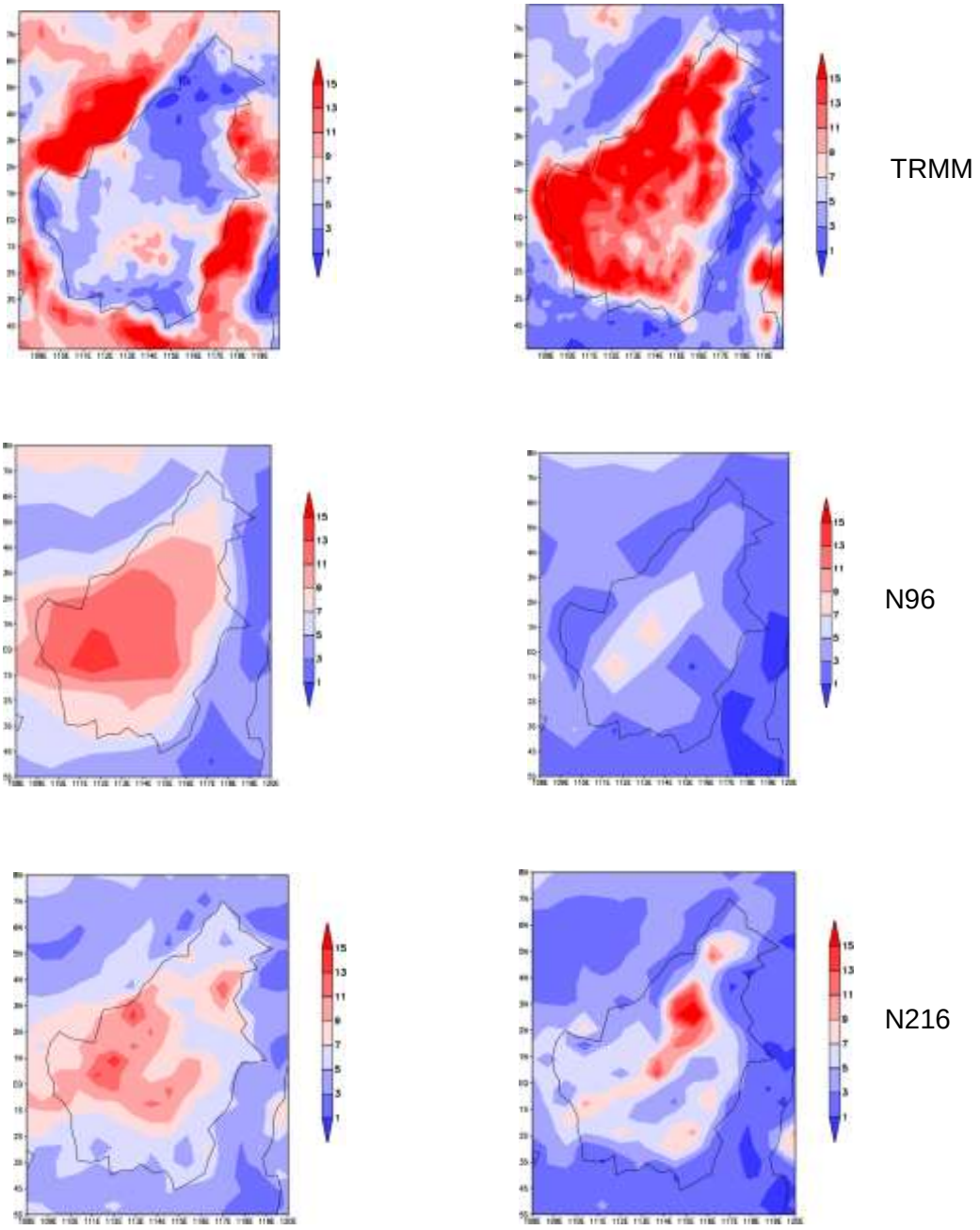

Figure 7 Morning (left) and evening (right) rainfall rate (mm/day) for TRMM observations, and model simulation in GA7.1 model with N96 and N216 resolutions.

Figure 7 shows the precipitation map at 8am and 8pm for the observation and model simulations. In the morning, the convection is already well developed in the model simulation, while the observed convection is still active around the coastal lines. In the evening the modelled inland convection is relatively weak because of lack of convective instability. This contrasts with the TRMM observations that show that the convection is able to maintain its intensity over the main land region in the evening time.

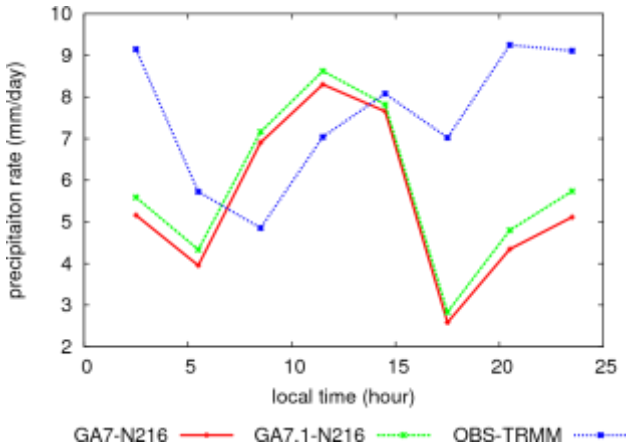

Figure 8 Diurnal cycles of the rainfall rate (mm/day) over Borneo island with N216 resolution for GA7 and GA7.1 models.

The diurnal cycle in GA7.1 is very similar to GA7 model except for a slight difference in the amplitude as shown in Figure 8. As pointed out earlier, CAPE closure tends to release the instability when it is available. Without changing CAPE closure, the convection still occurs too early in the higher resolution ACCESS model, reaching the maximum around midday instead of the evening/night as observed.

3.3 Sensitivities to convection changes

As discussed above, the diurnal cycle over tropical land remains poorly represented in GA7 and GA7.1. A potential source of these errors is that the convection scheme is too tightly coupled to the surface fluxes and CAPE, and too weakly coupled to the large-scale dynamics. Martin Willett and Whitall (2017) presented a simple modification that allows the deep convective entrainment rate to remain within a realistic range of values but be driven by the amount of convective activity within the last several hours, as measured by a 3-dimensional prognostic field based on surface convective precipitation. The underlying premise of the modification is that locations that have experienced high levels of recent convective activity will be populated with relatively large convective clouds that have low entrainment rates: conversely, locations that have experienced low levels of recent activity will be populated with relatively small convective clouds (if any) that will have high entrainment rates.

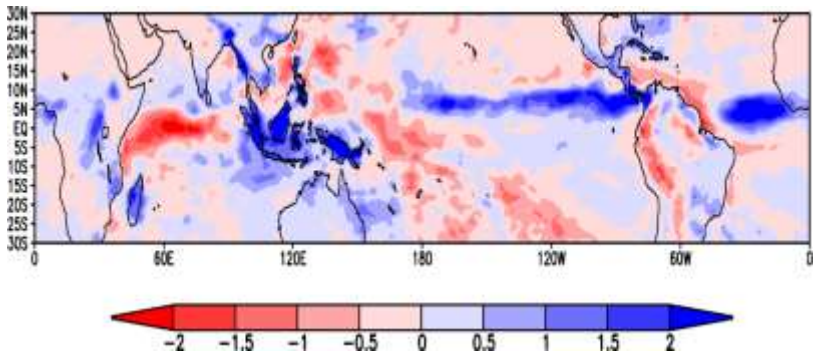

Figure 9 the difference in annual mean rainfall rate (mm/day) in GA7.1 model between the simulations with and without the convective memory change. (10y, from 1989-1998, unit: mm/day)

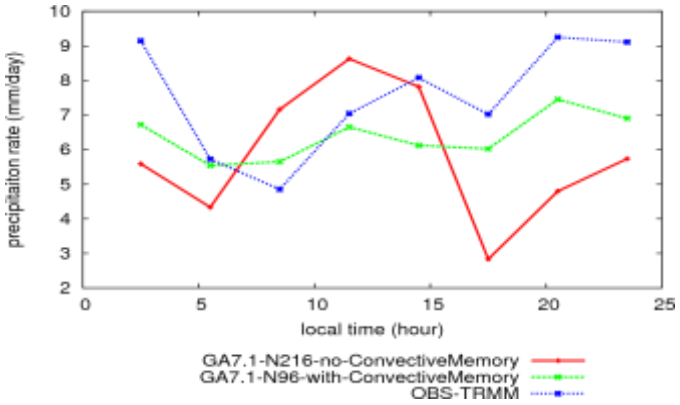

Figure 10 Diurnal cycles of the rainfall rate (mm/day) over the Borneo Island with N216 resolutions for GA7.1 model at N96 resolution with and without the convective memory change.

By implementing the convective memory change in GA7.1 model, the dry bias over the MC region is reduced (see Figure 9). The dry bias over Maritime Continent region (MC) and the wet biases over the Indian Ocean and West Pacific ocean are related through Walker circulation. Reducing dry bias over MC is accompanied with reduced wet biases over the oceans to the east and west (Zhu et. al. 2017). Due to a better coupling with the large scale dynamics, the diurnal cycle of rainfall rates also is much improved with more persistent convection over the land in the late afternoon and evening (see Figure 10).

Though the rainfall rate over the tropics has been improved, the rainfall biases are not completely alleviated. Figure 11 shows the rainfall rate bias for the experiment with convective memory change added in GA7.1. There are still wet bias over the western Indian Ocean and Eastern Pacific Ocean region. The dry bias has changed to wet bias over the MC land regions, but the dry bias remains in the surrounding ocean. The lag correlation of equatorial intraseasonal bandpass filtered OLR signals (Figure 12) shows slightly westwards propagation, which is not realistic. Further analysis and improvement of the change aims to be documented in a future work.

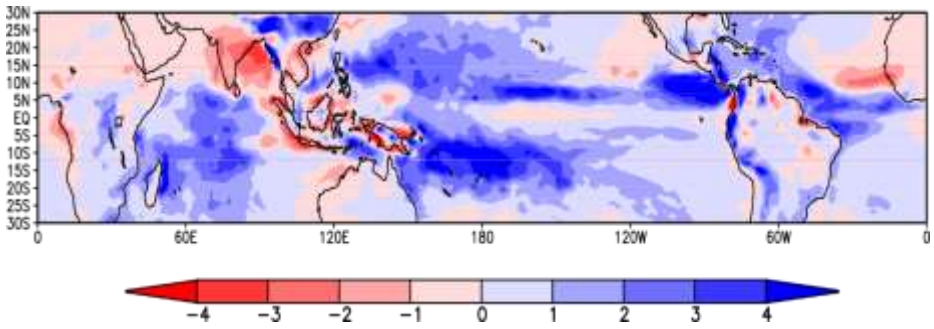

Figure 11 the annual mean rainfall rate (mm/day) bias for the experiment in N96 GA7.1 model with the convective memory changes comparing to GPCP rainfall estimate.

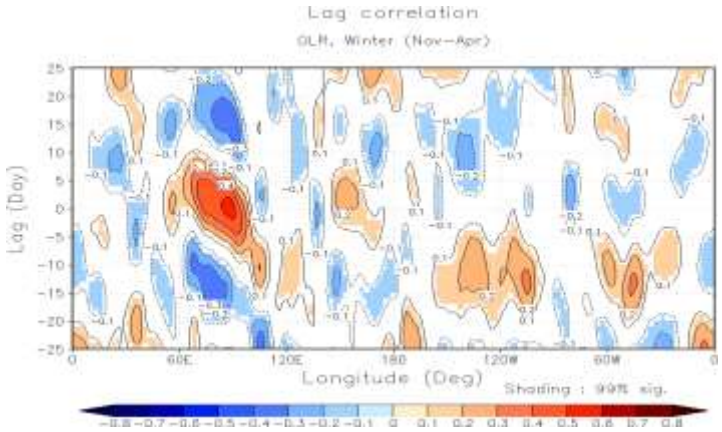

Figure 12 the lag correlation of equatorial intraseasonal OLR onto a reference zonal OLR time series at 90E for the N96 GA7.1 model simulation with convective memory changes.

3.4 Sensitivity to rainfall over land

As discussed earlier, ACCESS climate models have large positive systematic rainfall errors over the Western Indian and Western Pacific Ocean with a negative error over the Maritime Continent. To reduce the rainfall bias over the Indo-Pacific region, we also conducted sensitivity studies that increase the likelihood of convection to be triggered over land. To do so we add a positive temperature perturbation to the updraft parcel calculation in the convection code for all the grid points. We then carry out an ensemble of 4-months simulations initialized on 1 November, the start of warm seasons in the south hemisphere, of the years 2006 to 2010. Figure 13 shows the effect of this modification on the model rainfall climatology. Rainfall over land is increased, especially over the Maritime and African Continent, while rainfall over the Western Indian Ocean and the Western Pacific are reduced, especially in the SPCZ region. This is an encouraging result that we are currently investigating further. It also confirms the likely need to develop a parametrization for coastal convection. Work to do so is currently under way at Monash.

3.5 Evaluation of GA7.1 AMIP surface fluxes

3.5.1 Meridional distribution of the zonal-mean fluxes.

Momentum and energy exchanges between the surface and the atmosphere are crucial to climatic dynamics. Realistic representation of the exchanges is essential to a valid climatic modelling system.

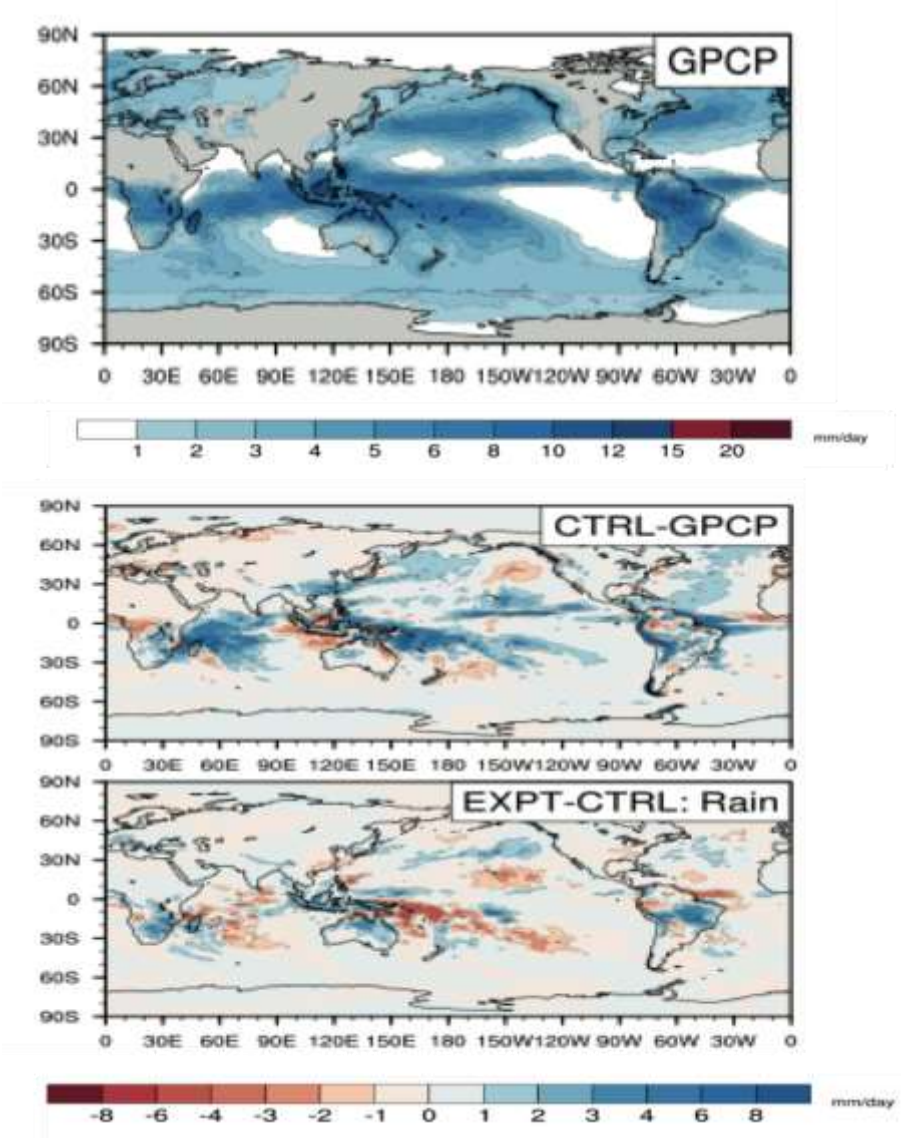

Figure 13 Observed DJF rainfall (top), Rainfall errors of the control (middle) and rainfall changes in the experiment (bottom). See text for details. (GA6 model physics).

Figure 14 shows meridional profiles of the zonal averaged surface fluxes and surface wind components of N96 GA7.1 AMIP run as described above. For the sensible heatflux, the GA7.1 AMIP results show good agreements with MERRA, ERA-INT, CFSR fluxes (within ±10 W/m^{2}in the northern hemisphere and at latitudes < 60˚S in the southern hemisphere), but are systematically larger than the NCEP2 flux, especially over the high latitudes and polar regions. Over Antarctica and its surrounding oceans (latitudes>60˚S), the modelled downward transferred sensible heat flux is underestimated against all the reanalyses, especially for NCEP2 and CFSR. For the latent heat flux,

the GA7.1 AMIP results also show good agreement with all the reanalyses at high latitudes (>50˚S and 50˚N). The differences between the GA7.1 AMIP and the MERRA, ERA-INT reanalyses profiles are within ±10 W/m^2. On the equator itself the fluxes from all the reanalyses and the GA7.1 AMIP runs are in good agreement.

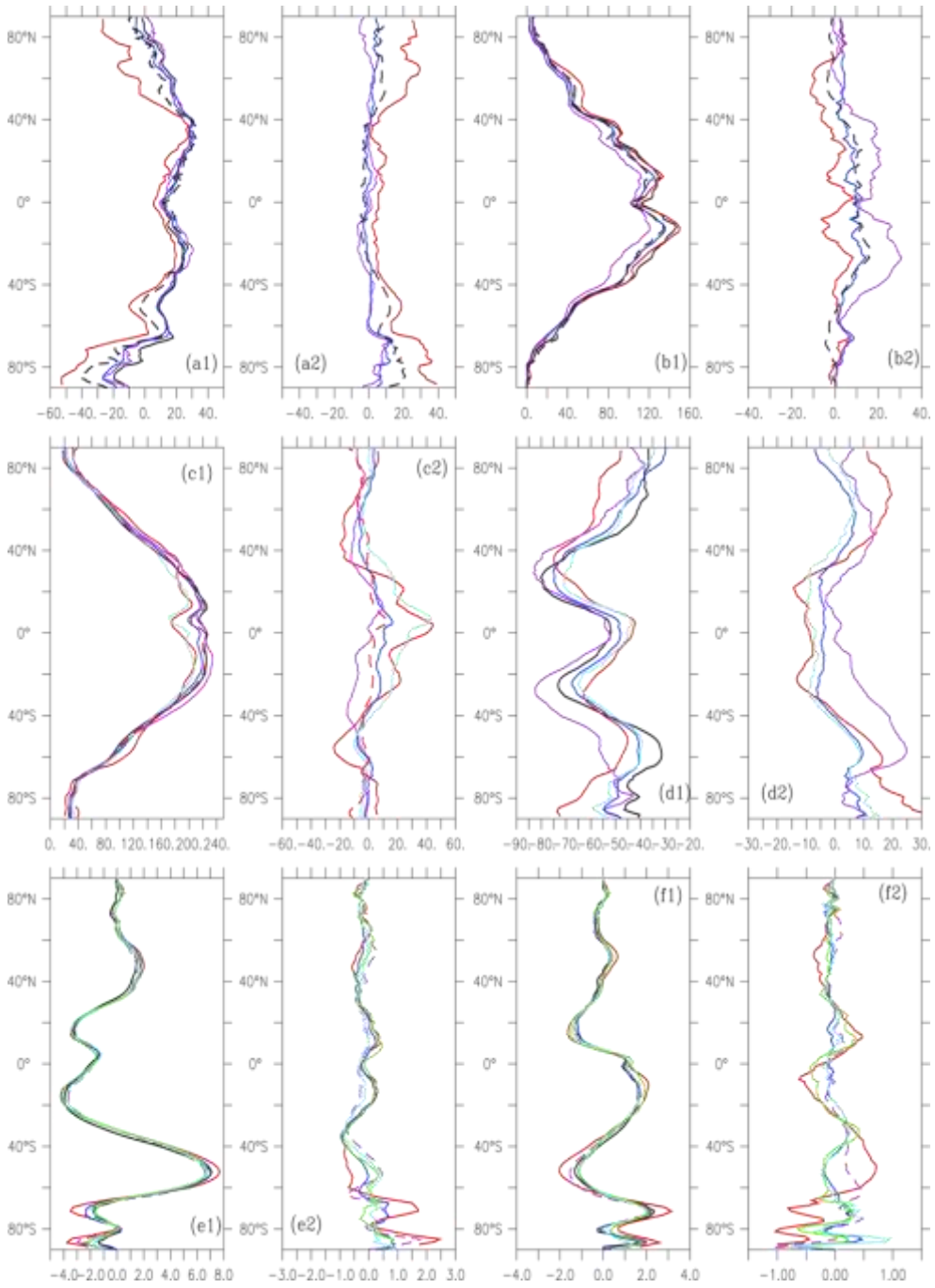

Figure 14 Meridional profiles of zonally averaged (a) sensible heat, (b) latent heat, (c) net shortwave radiative, (d) net longwave radiative fluxes at the surface (W/m^2), and surface (e) zonal, (f) meridional wind (m/s). Profiles in the frames with subtitle (1) denote the field from N96 GA7.1 AMIP runs (black solid line), the comparison reanalysis data sets of MERRA (solid purple line), NCEP2 (solid red line), ERA-INT (solid blue line), ERA40 (solid light blue line), COREV2 (solid green line), CFSR (dashed black line), JRA25 (dashed purple line), and the observational shortwave radiation data of SRB (solid red line). Profiles in the frames with subtitle (2) denote the difference between the field from N96 GA7.1 AMIP runs and the one from the comparison data sets (with the above defined colour/labelling).

For the shortwave radiative (SW) flux at the surface, at high latitudes there is close agreement between all the reanalysis products, the SRB observational data set, and the GA 7.1 AMIP simulation. For low to mid latitudes, there is considerable spread in the reanalyses and SRB observations, however, the agreement between model simulation and SRB observations remains close. Indeed, across all latitudes, the difference between the model simulation and SRB observations remains within +/- 15 W/m2, which is less than the model "error" measured against any of the reanalyses (Figure 14c2).

Similar results are also shown in the net longwave radiative (LW) flux comparison (Figure 14d1 and 14d2). Amongst all the reanalyses, the model "error" is least when measured against ERA-INT. The SW from the reanalysis data ERA-INT is very close to the observational data SRB, which further demonstrates that ERA-INT is more a more reliable date source.

The profile of the zonal wind from the GA7.1 AMIP runs matches very closely with the profiles from all the reanalysis datasets for almost all latitudes, except over Antarctica where those from NCEP2 and JRA25 show larger easterly winds than the others. The differences between the GA7.1 AMIP and the reanalyses profiles are relatively small, mainly within ±0.5m/s, though around 0.75m/s in the high westerly wind zone over the southern oceans (~7m/s). For the meridional winds component, the profile from GA7.1 AMIP shows very good agreements with all the reanalyses profiles (mostly within 0.2m/s) in the northern hemisphere, with the exception of NCEP2. Where significant biases occur, they are mostly in the southern oceans and Antarctica.

3.5.2 Global distributions of the mean fluxes

On average, sensible heat is transferred from the earth to the atmosphere in the low and mid-latitudes, and from the atmosphere to the earth in the polar and high latitude regions (Figure.15a). The Antarctic continent is a sensible heat sink for all the three distributions shown in Figure 15a1-3, but this sink is weakest in GA7.1 AMIP. In the distribution for GA7.1 AMIP small scattered heat sink patches appear in the middle of the southern oceans. These patches also appear in the ERA-INT distribution, but are much large in the NCEP2 distribution. As major moisture sources to the atmosphere, the tropical and low latitude oceans supply the largest latent heat flux. As shown in Figure. 15b1-3, those regions are also where there is the largest differences between the GA7.1 AMIP, NCEP2 and ERA-INT distributions. On the equator, the differences are relatively small.

Figure 15c5 shows that the Southern Ocean SW positive biases almost disappear in the GA7.1 AMIP simulations (Figures 15c4 and c5). This is a remarkable improvement comparing to results from the earlier versions of model, which could lead to a significant improvement in the SST simulation by a coupled model.

There are strong similarities in the global distribution patterns of both the zonal and meridional surface winds from GA7.1 AMIP and the other two reanalyses data sets (Figure 16e and f). These include the strong westerly over the southern oceans with the high centred in the southern Indian Ocean, and strong easterlies in the tropical and low latitudes caused by the subtropical Highs arising through descendent motions of the Hadley Cells.

3.5.3 The high resolution N216 GA7.1 AMIP test

We further evaluate the mean surface fluxes and surface winds from runs with the higher-resolution version (N216) of GA7.1 AMIP. Here we compare the simulated shortwave radiation with SRB data, and the other fields are compared with ERA-INT. As shown in Fig. 17a, the increased spatial resolution in the N216 GA7.1 AMIP improves the meridional profile of the zonally averaged sensible heat flux in the Polar Regions. Here differences appear on the edges of Antarctic continent where relatively large positive biases occurring in the N96 simulation are greatly reduced in the N216 simulation. Over the Arctic region, the positive bias in sensible heat flux in the N96 simulation is slightly reduced in the N216 simulation. As shown in Fig. 17b, N216 GA7.1 AMIP runs perform unevenly in improving meridional profile of the mean latent heat flux. The N216 runs mitigate the positive biases of the flux from the N96 runs at the polar latitudes; even eliminating the biases over the Antarctic regions. The biases around the edges of the continent are much reduced. However, the biases are increased in the equatorial and southern middle latitude oceans.

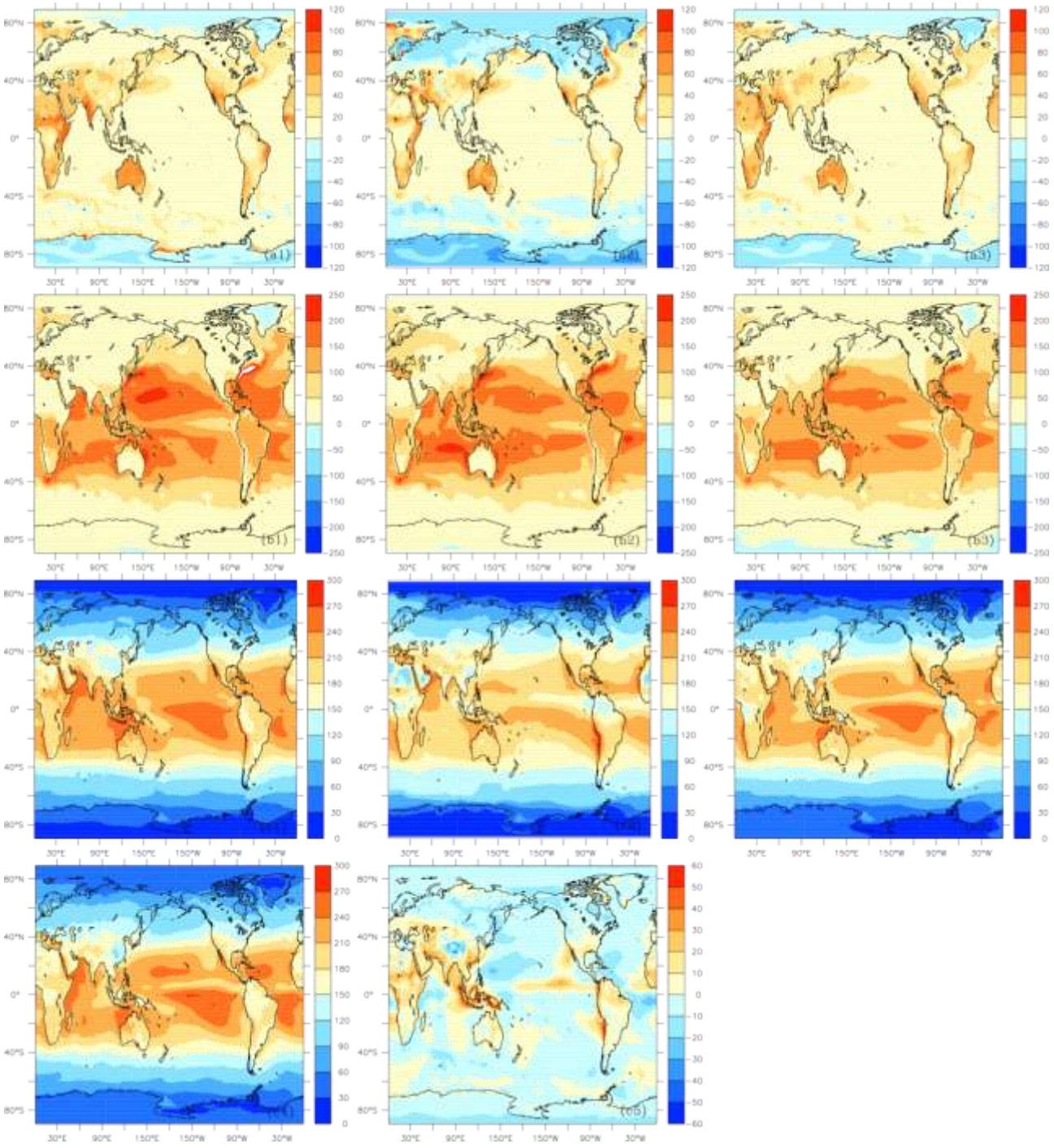

Figure 15 Global distributions of the surface fluxes and from N96 GA7.1 AMIP runs, the selected reanalyses and the observational data sets. The distributions are shown with (a) the sensible, (b) the latent heat flux and (c) the net long wave radiative flux (W/m2) at the surface from (1) N96 GA7.1 AMIP runs, (2) NCEP2 and (3) ERA-INT reanalyses. The observational net short wave radiative flux from SRB and the difference of the flux from N96 GA7.1 AMIP runs to the one form SRB are shown in (c4) and (c5), respectively.

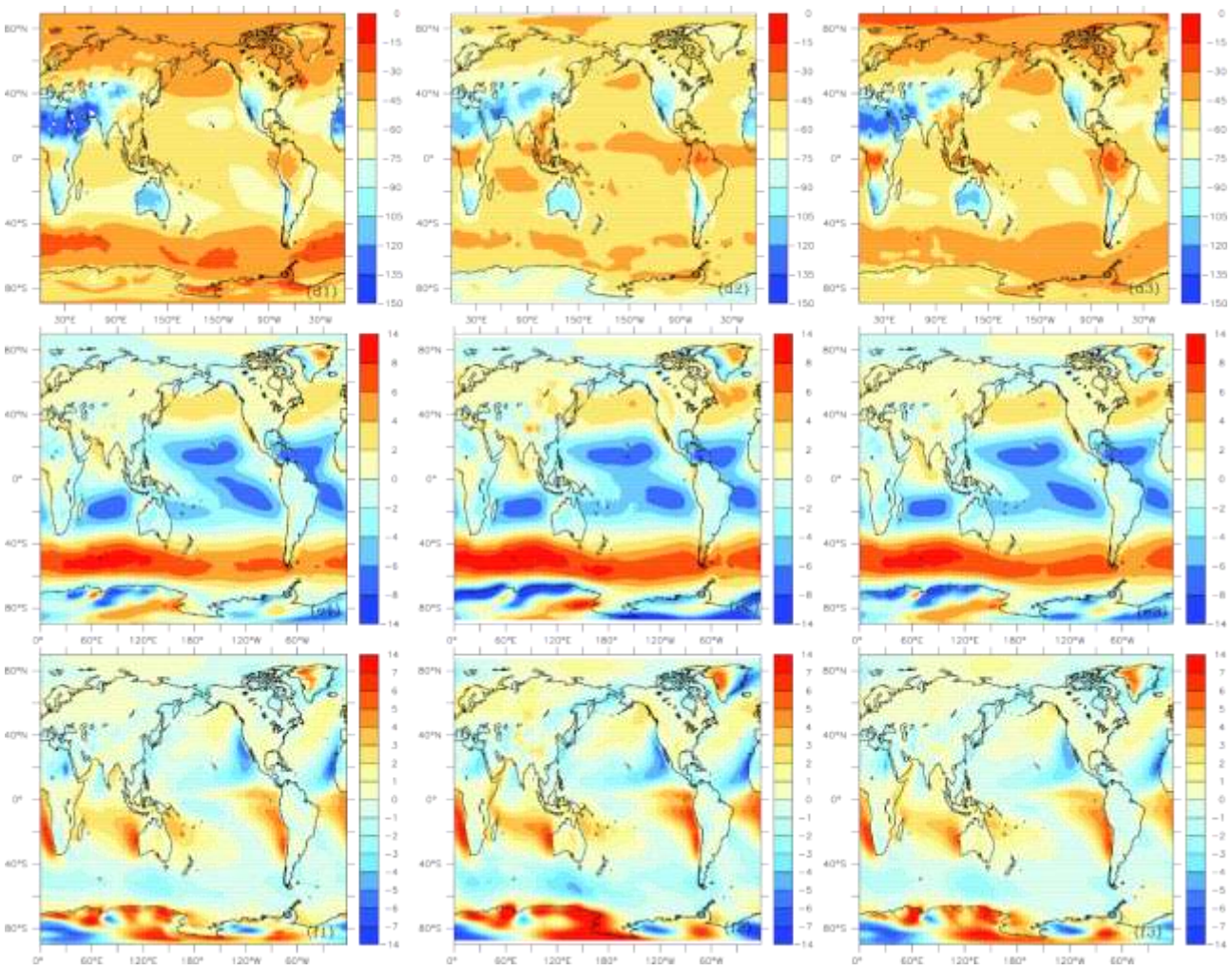

Figure 16 Global distributions of the surface fluxes and the surface winds from N96 GA7.1 AMIP runs, the selected reanalyses and the ERA-INT reanalyses. The distributions are shown with (d) the net longwave radiative flux at the surface (W/m2), (e) the surface zonal and (f) meridional wind (m/s) from (1) N96 GA7.1 AMIP runs, (2) NCEP2 and (3) ERA-INT reanalyses.

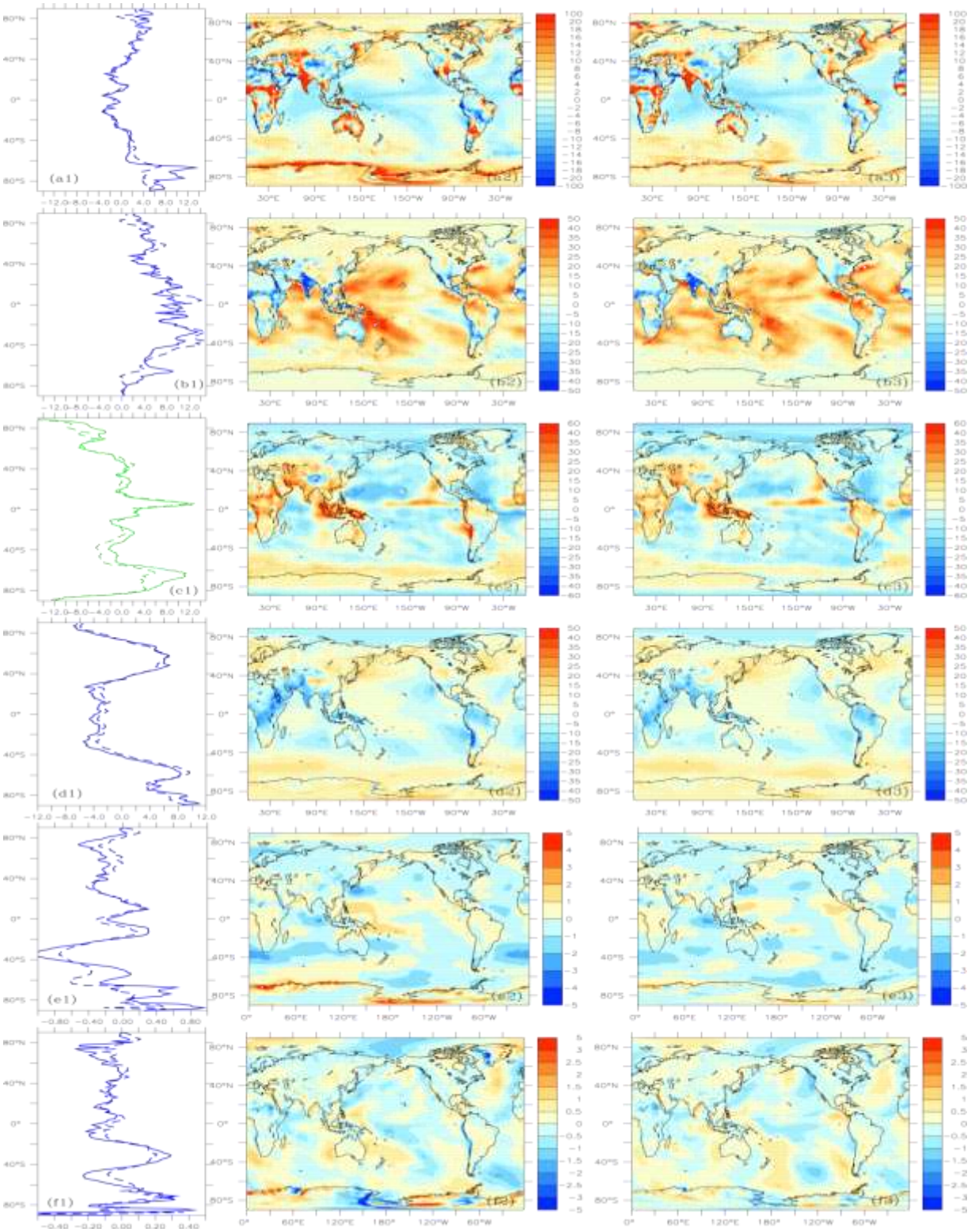

Figure 17 Comparisons of the mean surface fluxes and surface winds from N96 and N216 GA7.1 AMIP runs. Subtitles (a),the surface sensible, (b) latent heat, (c) net shortwave, (d) longwave radiative flux,€ zonal wind and (f) meridional wind .. Subtitle (1) denotes the differences of the zonal mean flux or wind from N96 GA7.1 AMIP (N216 GA7.1 AMIP) runs to the one from ERA-INT reanalyses with solid (dashed) blue line. Subtitle (2) and (3) denotes the difference of the flux or the wind global distribution from (2) N96 GA7.1 AMIP or (3) N216 GA7.1 AMIP runs to the one from ERA-INT reanalyses. In (c) the differences are to the shortwave radiative flux from observational SRB data set (green lines). Unit for the flux is (W/m2) and unit for the wind is m/s.

Fig 17c shows that the net downward solar radiative flux is improved with the N216 runs in the southern hemisphere, especially in the southern high latitudes, which would tend to favour the easing the southern ocean warm bias of sea surface temperature that widely exists in coupled climate models. The N216 simulation shows some mitigation of overestimated intakes of solar heating in the N96 simulation in the oceans off Peru and Chile coasts, and off the West African coast around 20 ˚S. It also shows mild mitigation of the overestimated flux in the maritime continent in the Asian tropics. As shown in figure 17d, the N216 simulation of the meridional profile of the mean longwave radiative flux has less bias than the N96 one almost along all the latitudes except the southern oceans (40-60 ˚S), although the differences of the biases are relatively small. The biases are notably reduced in regions around the Ross Sea in Antarctica, some large bias centres over oceans, and interestingly a spot on the northern part of Capsule Sea.

The improvement to the simulated surface winds from N216 GA7.1 AMIP is evident in Antarctica for both the zonal and meridional wind components (Fig. 17e, f). The N216 simulation reduces the large biases on the edges of the continent with steep topography and the large biases on the central ridge over inland Antarctica. Effects of subgrid orography induced wave drag and form drag, which is not well represented in climate models, are reduced in the high-resolution version N216 of GA7.1 AMIP model. We attribute the improvement of the surface wind simulation to these reduced dependency on the parameterised component of drag.

4. Single column model results

In this report, the ACCESS Singular Column Model (SCM) with GA6 physics is also used to identify and test possible modifications to the model representation of tropical convection with an aim to reduce model systematic errors.

4.1. Convective triggering

A major well-known flaw of the UM is its highly noisy (in time) triggering of deep convection. This has been a long-standing issue and has been attributed primarily to the closure assumption under deep convection. However, our investigations also revealed that the decision-making model for the occurrence of convection (the trigger function) has design limitations that might contribute to the noise.

In response, we have implemented a different trigger model, based on the work of Jakob and Siebesma (2003). Contrary to the current model's buoyancy-based triggering, the new model is based on the ascending parcel's vertical velocity. The parcel is assigned temperature and humidity perturbations at the surface, which are based on the strength of the turbulent surface fluxes. Then, an entraining plume set of equations is solved, including an equation for vertical velocity. If the vertical velocity at cloud base is upward, convection is deemed to occur, and the cloud top is determined as the first level above cloud base where the vertical velocity reduces to zero.

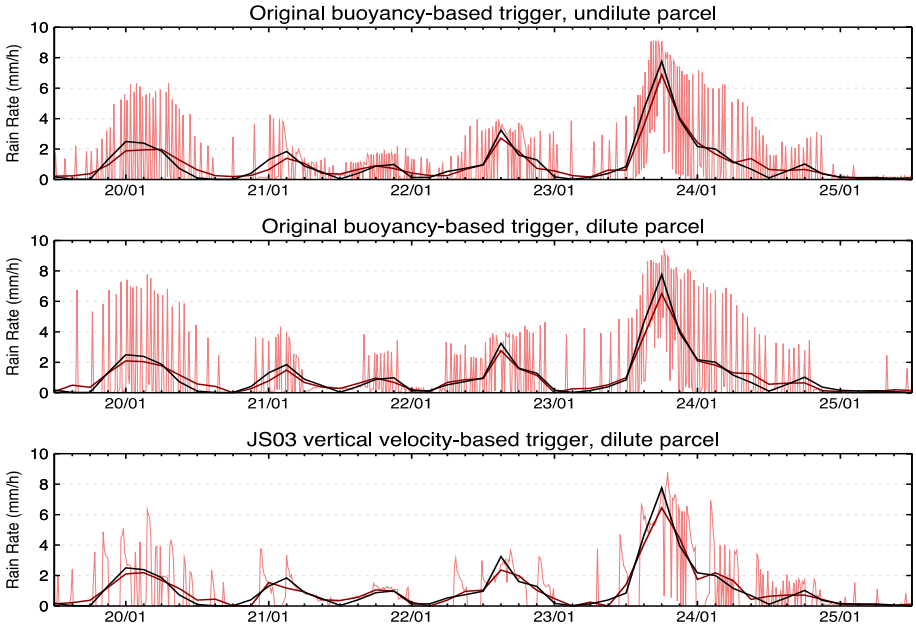

Figure 18 Rainfall in the TWP-ICE simulation of the GA6 SCM for the control model (top), the control model with a dilute parcel (middle) and the new vertical velocity trigger (bottom). Red line is for the time-step rainfall, black line is for 3-hourly observed rainfall rates and think red line is for the 3-hourly model averaged rainfall rate.

The Tropical Warm Pool International Cloud Experiment (TWP-ICE) was a field campaign which took place around Darwin in January and February 2006. SCM simulations were performed for the period 03 UTC, 17/01/2006 to 21 UTC, 12/02/2006 with the domain centred on the Darwin ARM site. Initial conditions and large-scale forcing were taken from the observational dataset. Horizontal advective tendencies for temperature and moisture were prescribed but the vertical terms were calculated by the model using the observed vertical velocity profile. Applying this change in the SCM TWP-ICE case demonstrates that the noise in convective triggering is significantly reduced (Figure 18). As is evident from the Figure the control simulations both with an undiluted and diluted trigger parcel show significant time-step to time-step noise in rainfall (thin red line), while the new trigger significantly reduces the noisy behaviour. Note that differences in 3-hourly average precipitation (black line = observed, thick red line = model) are small, as those are controlled by the large-scale forcing of the model.

4.2 Sensitivity to shallow convection

Another potential reason for the large positive rainfall biases of the tropical oceans is that there is too large a water transport from the sub-tropics into the tropics – in other words too much fuel (water) is supplied to the fire (tropical deep convection). Much of the water vapour that ultimately becomes rain in the tropics is extracted by evaporation over the sub-tropical oceans and transported into the tropics by the trade winds. Due to the strong feedbacks between convection and the circulation, subtle differences in the evaporation can lead to large changes in tropical rainfall (Tiedtke et al., 1988).

Evaporation in the trades in turn is strongly controlled by the strength of shallow convection. This can be understood through the role of shallow convection in entraining dry air from above the boundary layer by exchanging mass trough the trade inversion. The strength, defined as the mass-flux carried by the shallow clouds, of shallow convection affects this exchange in two ways. First, stronger convection simply exchanges more mass through the inversion, thereby increasing the import of dry air from above, which in turn increase the evaporation. Second, stronger convection will detrain more liquid water into the inversion, where it evaporates. The cooling from the evaporation will in turn weaken the inversion leading to a growth in the depth of the boundary layer (Stevens, 2007). Due to the strong vertical gradient in atmospheric humidity above the inversion, deeper cloud layers will entrain drier air from above, once again increasing evaporation.

To investigate the effects of shallow convection on the UM systematic rainfall biases, we are in the process of constructing a set of sensitivity studies that aim at varying the strength of shallow convection in the model. We begin our investigations by changing the mass-flux at cloud base when shallow convection is active in the model. Figure.19 shows some preliminary results of doing so in the SCM for a two-day idealized simulation of subtropical shallow convection. The Figure shows results from three experiments: i) a GA6 control, ii) the GA6 model with a trigger function that allows

for the dilution of the parcel as it rises, and iii) version ii) with a reduction in the shallow convective cloud base mass flux to 80% of its default value.

We carried out the SCM simulations using an idealised shallow cumulus test case (Grant and Lock, 2004). A fixed surface temperature (301 K), and roughness lengths for momentum and temperature (1.5 x 10-4 m and 1.5 x 10-5 m respectively) were used in the simulations. Because the initial wind profiles were not in geostrophic balance, the wind evolved throughout the simulations. The synthetically created idealised forcing profiles were used. The method for obtaining the forcings and initial conditions can be found in Grant and Lock (2004).

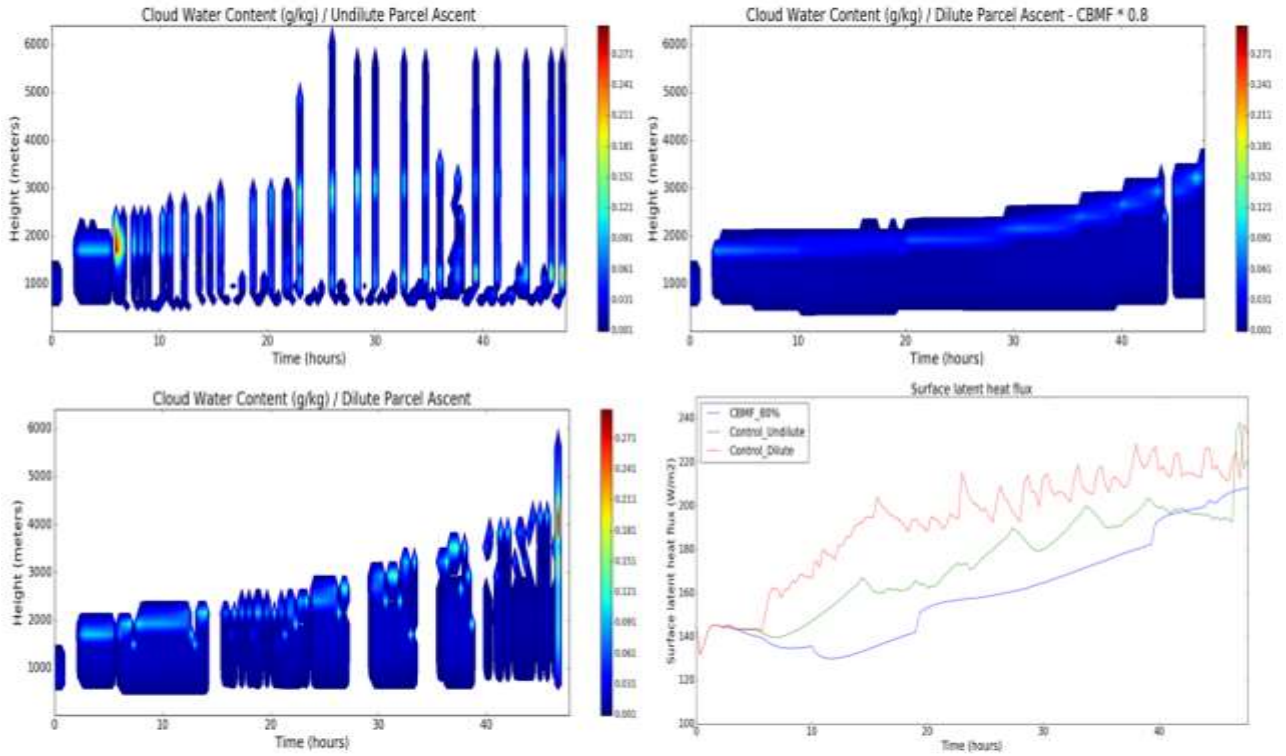

Figure 19 Cloud water content in the control (top left), dilute parcel (bottom left) and dilute parcel with reduced mass flux (top right) experiments as well as latent heat fluxes (bottom right). See text for details.

The control experiment develops deep convection when it should not and as a result, it cannot be used for our studies (Figure.19, top left). Replacing the undiluted parcel updraft in the trigger function with a dilute version, which is physically more realistic, alleviates this problem (Figure.19, bottom left), so our further experiments will use this version as their control. Reducing the cloud base mass-flux has the expected effect. It reduces the depth of the cloud layer (Figure.19, top right) and as result less dry air is entrained into the cloud layer. This leads to the expected reduction on latent heat flux (Figure.19, bottom right).

A drawback of the SCM approach is that there is no feedback to the large-scale circulation. The next step is therefore to investigate the impact of reducing the mass-flux in the full model. Experiments to do so are underway. The research work related to SCM simulations is future work on the model development than cataloguing current systematic errors.

5. Conclusions

Model systematic errors in the recent versions of the ACCESS climate model with GA7 and GA7.1 atmosphere model physics are compared and documented in this work. The evaluation of model bias is focused primarily in the following areas: tropical rainfall biases and MJO simulation; diurnal cycle; sensitivity to modification of convection scheme; surface heat fluxes and radiation fluxes.

For the tropical rainfall, the biases in GA7.1 are similar to that in GA7 model, with dry bias in the MC region and wet bias to the east and west ocean regions. By increasing model resolution, the rainfall bias in the Tropics is reduced in both GA7 and GA7.1 models, which in turn leads to improved MJO simulation.

Capturing the diurnal cycle has been a challenging topic for AGCMs. The diurnal cycle in both the GA7 and GA7.1 models, peaks too early due to the design of the convection scheme, which does not allow for convective instability to properly accumulate. The diurnal cycle simulation over the MC land region is improved in the N216 model in terms of the timing of peak rainfall, and its amplitude, improvement we attribute to the better-resolved terrain in N216. Both N96 and N216 model simulations have weaker offshore convection than indicated by TRMM observations.

To improve the coupling between model convection and the large-scale dynamics, a "convective memory" scheme is introduced into the current convection parameterisation. This memory scheme ties the deep convection entrainment rate to a proxy for the amount of convective activity within the last several hours. Introduction of the convective memory scheme improves the model's diurnal cycle. It has significantly reduced the rainfall dry bias in magnitude over the MC. However, impact on the MJO simulation is negative, probably due to the change of the interaction between convection and large-scale dynamics. Further improvement is needed and that is a topic for future work.

The sensible and latent heat and net radiative fluxes at the surface, and surface wind components simulated by the N96 GA7.1 AMIP model show general similarity and consistency to their counterparts from well known and established reanalysis data sets, this consistency also holds in comparing GA7.1 simulated net shortwave radiative flux to the SRB observational radiation data set. Though the bias of net long wave radiative flux at the surface is relatively large, it is not judgemental given the large difference among the available reanalysis. The surface wind components are very close to the reanalyses in its meridional profile of the zonally averaged fields, as well as the global distribution patterns from the two selected reanalysis data sets (NCEP2 and ERA-INT). The high-resolution N216 GA7.1 AMIP model generally performs better than N96 GA7.1 AMIP model, in terms of the energy exchanges at the surface and the surface winds over the globe, especially in the vicinity of the Antarctic coastal margins.

The promising avenues for reducing the systematic errors identified from SCM experiments is increasing rainfall rate over land, most likely by introducing a parametrization of coastal convection as well as changing the strength of shallow convection. We will continue to investigate those while also making some improvements to the model, such as an improved convection trigger model. We are constructing an idealized case for deep convection, which aims at identifying convective equilibria and the processes that control them for different strengths atmospheric forcing. In this report, our SCM experimentation is limited to the GA6 version of the atmospheric model, but progress has been made to set up an SCM version for UM7.1.

6. References

Berrisford, P., D. Dee, K. Fielding, M. Fuentes, P. Kållberg, S. Kobayashi, and S. Uppala, 2009: ERA report series - The ERA-Interim archive Version 1.0. Weather, 16. http://www.ecmwf.int/publications/library/ecpublications/_pdf/era/era_report_series/RS_1.pdf.

Edwards, J. M. and Slingo, A., 1996: Studies with a flexible new radiation code. I: Choosing a conFigureuration for a large-scale model, Quart. J. Roy. Meteorol. Soc., 122, 689-719.

Gates, W. L., J. Boyle, C. Covey, C. Dease, C. Doutriaux, R. Drach, M. Fiorino, P. Gleckler, J. Hnilo, S. Marlais, T. Phillips, G. Potter, B. Santer, K. Sperber, K. Taylor and D. Williams, 1998: An Overview of the Results of the Atmospheric Model Intercomparison Project (AMIP I). Bull. Amer. Meteor. Soc., 73, 1962-1970.

Gregory, D and Rowntree, P. R., 1990: A mass-flux convection scheme with representation of cloud ensemble characteristics and stability dependence closure. Mon. Weather Rev., 118:1483-1506.

Grant and Lock, 2004: The turbulent kinetic energy budget for shallow cumulus convection, Q. J. R. Meteorol. Soc. (2004), 130, pp. 401–422.

Huffman, G. J., Adler RF, Morrissey M, Bolvin DT, Curtis S, Joyce R, McGavock B, Susskind J. 2001. Global precipitation at one-degree daily resolution from multi-satellite observations. J. Hydrometeor. 2: 36–50.

Huffman, G.J., R.F. Adler, D.T. Bolvin, G. Gu, E.J. Nelkin, K.P. Bowman, Y. Hong, E.F. Stocker, D.B. Wolff, 2007: The TRMM Multi-satellite Precipitation Analysis: Quasi-Global, Multi-Year, Combined-Sensor Precipitation Estimates at Fine Scale. J. Hydrometeor., 8:38-55

Jakob, C., and A. P. Siebesma, 2003: A new subcloud model for mass-flux convection scheme: Influence on triggering, updraft properties and model climate. Mon. Wea. Rev, 131, 2765–2778.

Jourdain, N.C., Sen Gupta, A., Taschetto, A.S., Ummenhofer, C., Moise, A.F., Ashok, K. (2013).The Indo-Australian monsoon and its relationship to ENSO and IOD in reanalysis data and CMIP3/CMIP5 simulations, Climate Dynamics, 41, 3073-3102

Kanamitsu, M., W. Ebisuzaki, J. Woollen, S.-K. Yang, J. J. Hnilo, M. Fiorino, and G. L. Potter, 2002: NCEP–DOE AMIP-II Reanalysis (R-2). Bull. Am. Meteorol. Soc., 83, 1631–1643, doi: 10.1175/BAMS-83-11-1631. http://journals.ametsoc.org/doi/abs/10.1175/BAMS-83-11-1631.

Kettle, A. J., Andreae, M. O., Amouroux, D., Andreae, T. W., Bates, T. S., Berresheim, H., Bingemer, H., Boniforti, R., Curran, M. A. J., DiTullio, G. R., Helas, G., Jones, G. B., Keller, M. D., Kiene, R. P., Leck, C., Levasseur, M., Malin, G., Maspero, M., Matrai, P., McTaggart, A. R., Mihalopoulos, N., Nguyen, B. C., Novo, A., Putaud, J. P., Rapsomanikis, S., Roberts, G.,

Schebeske, G., Sharma, S., Simó, R., Staubes, R., Turner, S., and Uher, G.: A global database of sea surface dimethyl sulfide (DMS) measurements and a procedure to predict sea surface DMS as a function of latitude, longitude, and month, Global Biogeochem. Cycles, 13, 399–444, https://doi.org/10.1029/1999GB900004, 1999.

Klingaman NP, Woolnough SJ. 2014. Using a case-study approach to improve the Madden–Julian oscillation in the Hadley Centre model. Q. J. R. Meteorol. Soc. 140: 2491–2505, doi: 10.1002/qj.2304.

Lana, A., Bell, T. G., Simó, R., Vallina, S. M., Ballabrera-Poy, J., Kettle, A. J., Dachs, J., Bopp, L., Saltzman, E. S., Stefels, J., Johnson,J. E., and Liss, P. S.: An updated climatology of surface dimethlysulfide concentrations and emission fluxes in the global ocean, Global Biogeochem. Cycles, 25, GB1004, https://doi.org/10.1029/2010GB003850, 2011.

Large, W. G., and S. G. Yeager, 2009: The global climatology of an interannually varying air - Sea flux data set. Clim. Dyn., 33, 341–364, doi: 10.1007/s00382-008-0441-3.

Liu, Y., Daum, P. H., Guo, H., and Peng, Y.: Dispersion bias, dispersion effect, and the aerosol-cloud conundrum, Environ. Res. Lett., 3, 045 021, 2008.

Lock, A.P., Brown, A.R., Bush, M.R., Martin, G.M. and Smith, R.N.B. 2000: A new boundary layer mixing scheme. Part I: Scheme description and single column model tests. Mon. Weather Rev., 128, 3187-3199.

Neale R. and Slingo. J (2002): The Maritime Continent and its role in the global climate: a GCM study. J. of Climate, Vol 16, 834-848.

ONOGI, K., and Coauthors, 2007: The JRA-25 Reanalysis. J. Meteorol. Soc. Japan. Ser. II, 85, 369–432, doi:10.2151/jmsj.85.369. https://www.jstage.jst.go.jp/article/jmsj/85/3/85_3_369/_article.

Peixoto, J. P., and A. H. Oort, 1992: Physics of Climate. Spring-Verlag, New York, 520 pp.

Rienecker, M. M., and Coauthors, 2011: MERRA: NASA's modern-era retrospective analysis for research and applications. J. Clim., 24, 3624–3648, doi:10.1175/JCLI-D-11-00015.1.

Saha, S., and Coauthors, 2010: The NCEP climate forecast system reanalysis. Bull. Am. Meteorol. Soc., 91, 1015–1057, doi:10.1175/2010BAMS3001.1.

Stevens, B., 2007: On the Growth of Layers of Nonprecipitating Cumulus Convection. J. Atmos. Sci, 64, 2916–2931, doi:10.1175/JAS3983.1.

Tiedtke, M., W. A. Heckley, and J. Slingo, 1988: Tropical forecasting at ECMWF: The influence of physical parametrization on the mean structure of forecasts and analyses. Quart. J. Royal Meteor. Soc, 114, 639–664, doi:10.1002/qj.49711448106.

Uppala, S. M., and Coauthors, 2005: The ERA-40 re-analysis. Q. J. R. Meteorol. Soc., 131, 2961–3012, doi:10.1256/qj.04.176. http://doi.wiley.com/10.1256/qj.04.176.

Walters, D., Baran, A., Boutle, I., Brooks, M., Earnshaw, P., Edwards, J., Furtado, K., Hill, P., Lock, A., Manners, J., Morcrette, C., Mulcahy, J., Sanchez, C., Smith, C., Stratton, R., Tennant, W., Tomassini, L., Van Weverberg, K., Vosper, S., Willett, M., Browse, J., Bushell, A., Dalvi, M., Essery, R., Gedney, N., Hardiman, S., Johnson, B., Johnson, C., Jones, A., Mann, G., Milton, S., Rumbold, H., Sellar, A., Ujiie, M., Whitall, M., Williams, K., and Zerroukat, M.: The Met Office Unified Model Global Atmosphere 7.0/7.1 and JULES Global Land 7.0 conFigureurations, Geosci. Model Dev. Discuss., https://doi.org/10.5194/gmd-2017-291, 2017.

Wilson, D. R., Bushell, A. C., Kerr-Munslow, A. M., Price, J. D., and Morcrette, 2008: A prognostic cloud fraction and condensation scheme. I: Scheme description. Quart. J. Roy. Meteorol. Soc., 134, 2093-2107.

Willett M. R. and M. A. Whitall, 2017: A simple prognostic based convective entrainment rate for the unified model: description and tests, Forecasting Research Technical report No: 617, UK Met Office.

Yang, G. and J. Slingo, 2001: The Diurnal Cycle in the Tropics, Monthly Weather Review, 129, 784-801

Zhu, H., E. Maloney, H. Hendon and R. Stratton, 2017: Effects of the changing heating profile associated with melting layers in a climate model. Quart. J. Roy Met. Soc. DOI:10.1002/qj.3166

Earth Systems and Climate Change Hub

National Environmental Science Programme

www.nespclimate.com.au